Effects of temperature on aging of closed-cell foam insulations and their temperature-dependent long-term thermal resistance

Kodippili, Dulani P. A.; Molleti, Sudhakar; Van Reenen, David; Drouin, Michel

STP1657 on Symposium on Changing Face of Building Materials and Systems in Response to Climate Change, 2025-04-09

Effects of Temperature on Aging of Closed-Cell Foam Insulations and Their Temperature-Dependent Long-Term Thermal Resistance

Dulani P. A. Kodippili[1], Sudhakar Molleti[2], David Van Reenen[3], and Michel Drouin[4]

ABSTRACT

The long-term thermal resistance of three polyisocyanurate (PIR) materials (PIR I, PIR II, and PIR III), extruded polystyrene (XPS), and medium density spray foam (MDSPF) were investigated using the accelerated aging procedures defined in slicing and scaling methods in CAN/ULC-ULC S770 and ASTM C1045 for the following effects.

1. The effect of conditioning temperature on the aging of closed-cell foams by evaluating the long-term thermal resistance (LTTR),
2. Temperature dependent R-value of closed-cell foams (TDRV).
3. Comparison of the TDRV measured as per ASTM C518 and calculated as per ASTM C1045 for 5 years-aged full thickness boards with that of the accelerated aged thin slices as per CAN/ULC-S770.

First, closed-cell insulations were tested following the methods in CAN/ULC-S770. In addition to conditioning at 23 °C, the thin slices were conditioned at -10 °C and 50 °C. The LTTR was calculated as per ULC-S770. The thermal conductivity was tested at multiple (10) mean

[1] Corresponding Author, National Research Council, Ottawa, ON, K1A 0R6, Canada; 0000-0002-9906-7314; Email: dulanipankaja.abeysingkodippili@nrc-cnrc.gc.ca
[2] National Research Council, Ottawa, ON, K1A 0R6, Canada; 0000-0001-5683-626X
[3] National Research Council, Ottawa, ON, K1A 0R6, Canada; 0009-0007-4953-562X
[4] Consultant for Polyiso Industry, Beloeil, Qc, J3G 5E8, Canada

temperatures in addition to the specified 24 °C mean temperature at the testing points. The TDRV of the accelerated aged samples (thin slices) was calculated as per ASTM C1045. Finally, the full thickness boards were conditioned in the laboratory for 5 years at -10 °C, 23 °C, and 50 °C. The TDRVs of the full thickness boards were compared with those of the thin slices.

The LTTR (at 24°C) by the accelerated testing shows biases towards the LTTR measured at 5 years. The biases range from -4.7 - 7.1%, 0.6 - 8.7%, and -0.9 - 12.5% when the specimens were conditioned at -10°C, 23°C, and 50°C respectively. The TDRVs of samples conditioned at 23 °C and 50 °C show very close values for accelerated aging and 5-year laboratory aging. Regardless, of the conditioning temperature, XPS aged similarly, reaching very similar TDRVs at 5 years and 5-year equivalent periods.

Keywords

Long-term thermal resistivity, LTTR, closed-cell foam insulations, polyisocyanurate, extruded polystyrene, polyurethane, temperature dependent thermal resistivity/conductivity.

Introduction

It is important to assess and predict the long-term thermal performance of building materials to design energy efficient, thermally comfortable, durable, and sustainable buildings. Closed-cell foam insulations are commonly used in building construction due to their comparably high thermal resistance values among the insulation materials. Therefore, their performance in the buildings play a crucial role when designing buildings. The thermal resistance of all insulations including the closed-cell materials is dependent on the temperature and material itself. The closed-cell foam insulations contain gases inside their closed-cells in the polymeric matrix. The gases are

called blowing agents (BAs). The high thermal performance of these materials come mainly from the specific blowing agents (BAs) that are inside the closed-cells. The BAs have a lower thermal conductivity than the air (N_2 and O_2) due to their high molecular weight. These BAs are intended to be retained in the structure of the foam. However, over time the air outside the material diffuses into the material and BAs diffuse out of the material. The inward diffusion occurs at a faster rate than the outward diffusion due to the reason that the molecular weights of the BAs are greater than the air [1, 2]. Specially molecules such as Nitrogen, Oxygen, Carbon Dioxide, and water vapour can diffuse at a faster rate compared to the BAs [2]. This results in declining the thermal resistance of closed-cell foam over time. This phenomenon is called thermal aging. Since the compositional changes occur in these materials, it is a challenge to accurately determine the thermal resistance values required for designing energy-efficient buildings. Therefore, it is important to develop proper test methods to predict the thermal performance of closed-cell foam insulations.

Polyisocyanurate (PIR), extruded polystyrene, and spray polyurethane foam are closed-cell foam materials that are commonly used as an insulating material in the construction industry, due to their high thermal insulating performance with their affordable cost. In addition to the thermal aging, BAs are subjected to phase changes due to temperature fluctuations. The temperature dependency of PIR is not linear and this behavior influences designers to use thicker layers of insulation[3]. There are two approaches used to evaluate the long-term thermal performance of insulation products. One approach is elevating the temperature to accelerate the diffusion-controlled thermal aging. In this approach, the changes in permeability, solubility coefficients, and diffusion characteristics with the temperature change are not considered for the evaluations[4]. The other approach is reducing the thickness of the tested foam layers to accelerate the aging process[4]. Some of the test methods are ASTM C1303/C1303M-23[5], CAN/ULC-S770-20[6] and

ISO11561:1999[7]. These methods utilize the accelerated aging process called slicing and scaling method in which the gas diffusion is accelerated by the slicing the full thickness material into thin slices. In this process, the relationship of the diffusion time and the distance is employed to determine the testing point for the sliced material.

The existing standard test methods to predict require the samples for the "slicing and scaling method" to be conditioned at the regular laboratory conditions such as ambient air at 23±5 °C temperature and 50±20% relative humidity. These ambient conditions are not intended to replicate actual use conditions, but for comparison of different materials. However, in reality insulation materials are exposed to a range of high and low temperatures during their service life. Also, at low temperatures the BAs start condensing which will increase thermal conductivity of the insulations. Overtime, the BAs can dissolve into some domains in the polymer, which will also increase the thermal conductivity of the closed-cell foams. The temperature variations affect both, the diffusion process and the solubility of the BAs. An investigation by Berardi[8] showed the impact of the elevated temperature, elevated humidity and freeze and thaw cycling on thermal aging of closed-cell foam insulation. Zhang et al.[9] investigated the influence of aging at alternate high and low temperatures (-40 °C and 70 °C for 12 hours each for a week), and aging at 40 °C for a week on the thermal conductivity of Polyurethane foams by using transient plane source method (TPS). They reported that the increase of thermal conductivity at 20 °C is 8-12% for the samples that had been aged at the alternate temperatures, while the increase is 1.6-3.8% for the samples that had been aged at 40 °C [9]. Therefore, it is important to account the effects of the temperature into the existing test methods.

The phase changes in some BAs at in-service temperature range increase the thermal conductivity of PIR at lower temperatures and result in a non-linear relationship between thermal

conductivity and temperature. Zhang et al.[9] pointed out that the boiling point of one of the BAs, HFC-245fa is 15.3 °C and starts condensing at 15.3 °C. The new generation blowing agents such as HFO-1336mzz-Z, HFO-1336mzz(E), HCFO-1233zd-E, n-pentane, iso-pentane, and cyclo-pentane have normal boiling points of 33.4 ºC[10, 11], 7.5 ºC[12], 18.0 °C[11], 36.1°C[13], 27.8°C[14], and 49.3°C[13] respectively. As the liquid phase of the BAs has higher thermal conductivity than the gaseous phase, the overall thermal conductivity of closed-cell foams with BAs could increase significantly at low temperatures.

This research investigates the LTTR of polyisocyanurate, extruded polystyrene, and polyurethane spray foam according to the ULC-S770 slicing and scaling method. In addition to that, the LTTR of the materials is calculated according to the ASTM C1303 method. The existing tests limit the conditioning of materials only at 23 °C. Therefore, the effect of the conditioning at -10 °C and 50 °C on the closed-cell foam insulations and how the conditioning temperature impacts on the accelerated testing method are studied. The LTTR test method requires conducting thermal transmission properties tests according to ASTM C518 or ASTM C177 test methods. These tests assume the thermal conductivity of the material is linear with temperature. However, the non-linear behaviour of the thermal conductivity of closed-cell insulations with temperature necessitates the use of the ASTM C1045 method to calculate its' thermal conductivity at a given mean temperature. Previous research[15, 16] showed how ASTM C1045 test method can be employed in the LTTR testing for closed-cell materials. In this study, the use of ASTM C1045 method for the LTTR testing is explored and the results are compared with the samples aged for 5 years.

Materials and Methods

MATERIALS

The materials used for this study are paper faced, Type 2 Class 2 (CAN/ULC-704.1) PIR boards from three different manufacturers, Type 4 (CAN/ULC-701.1) XPS board, and medium density spray polyurethane foam (CAN/ULC-705.1). The characteristics of the materials are given in Table 1.

Table 1: Properties of tested materials

Material	Type	Thickness (mm)	Density (kg/m^3)	Facer type	BA
PIR I	Type 2 Class 2	50.9 ±0.3	35.4 ±0.3	Paper	Pentane based
PIR II	Type 2 Class 2	53.5 ±0.3	35.2 ±0.3	Paper	Pentane based
PIR III	Type 2 Class 2	52.9 ±0.6	34.8 ±0.6	Paper	Pentane based
XPS	4	51.6 ±0.3	24.2 ±0.3	-	HFC based
MDSPF	Medium Density	foamed with a thickness > 60 mm and cut in to 50 mm thickness excluding the formed skin	35.4 ±2.0	-	HFO based

METHODOLOGY

The procedure of long-term thermal resistance (LTTR) testing

The long-term thermal resistance of the materials was tested as per CAN/ULC S770 and ASTM C518 test methods. Additional steps of testing were added to the testing procedure to investigate the effect of conditioning at different temperatures and to determine the temperature-dependent thermal properties. The full thickness boards were received at the laboratory within a week of manufacturing. The boards were conditioned in the laboratory for approximately 2 days at 23 °C and 50% RH. Three specimens of 600 x 600 mm were cut from the center of one board using a vertical band-saw. The initial thermal resistance of the specimen at the mean temperature of 24 °C was determined according to the ASTM C518 test method by using the FOX600 Heat

flow meter. Then, each 600 x 600 mm specimen was cut into quarters of 300 x 300 mm specimens. Three of the 300 x 300 mm specimens were sliced using a horizontal bandsaw to obtain 10 mm thick slices/specimens and one 300 x 300 mm specimen was retained for each 600 x 600 mm specimen. The thicknesses of the sliced specimens and the full thickness specimens were measured using a Mitutoyo digimatic indicator with a resolution of 0.01 mm as specified in CAN/ULC S770. Two stacks of 10 mm thin slices were separated as four core slices and four surface slices from each 600 x 600 mm specimen (Set 1, made of a stack of 4 core slices and a stack of 4 surface slices). Two similar stacks (Set 2 and 3) were also prepared. The thermal resistivity of set 1 (stack of core slices and stack of surface slices) were tested according to ASTM C518 at 24 °C mean temperature simultaneously by using FOX314 Heat flow meter. In addition to the steps of testing in the CAN/ULC S770 test method, the thermal resistivity of the retained 300 x 300 x 50 mm specimen was tested at eleven mean temperatures as per ASTM C518. The mean temperatures of testing, the cold plate temperatures, and the hot plate temperatures used in the testing are given in Table 2. The temperature set points were determined based on ASTM C 1058. The aging period for the 10 mm thin slices was calculated using the scaling equation (Equation 1) for the equivalent of 5 years of aging for the full thickness product. The mean thickness of the 10 mm thin slices and the mean thickness of the full thickness board were used for the calculation. The three sets (Set 1, 2, and 3) of core slices and surface slices, and the full thickness specimen from each 600 x 600 mm specimen were conditioned at -10±3 °C, 23±1°C, and 50±1°C respectively. At the end of the calculated aging period equivalent 5 years for the slices, the thermal resistivity of the slices was tested according to ASTM C518 at eleven mean temperatures listed in (Table 2). The full thickness board was tested at the end of conditioning for 5 years. The test was carried out according to ASTM C518 at eleven mean temperatures listed in (Table 2). This procedure is shown in **Error!**

Reference source not found..

Table 2: Temperature setpoints for testing

Set points for heat flow meter (°C)		**Mean temperature (°C)**	**Temperature difference (°C)**
Hot plate	**Cold plate**		
0	-20	-10	20
12	-20	-4	32
20	-20	0	40
24	-15	5	39
24	-4	10	28
26	4	15	22
31	9	20	22
35	13	24	22
44	20	32	24
52	24	38	28
64	24	44	40

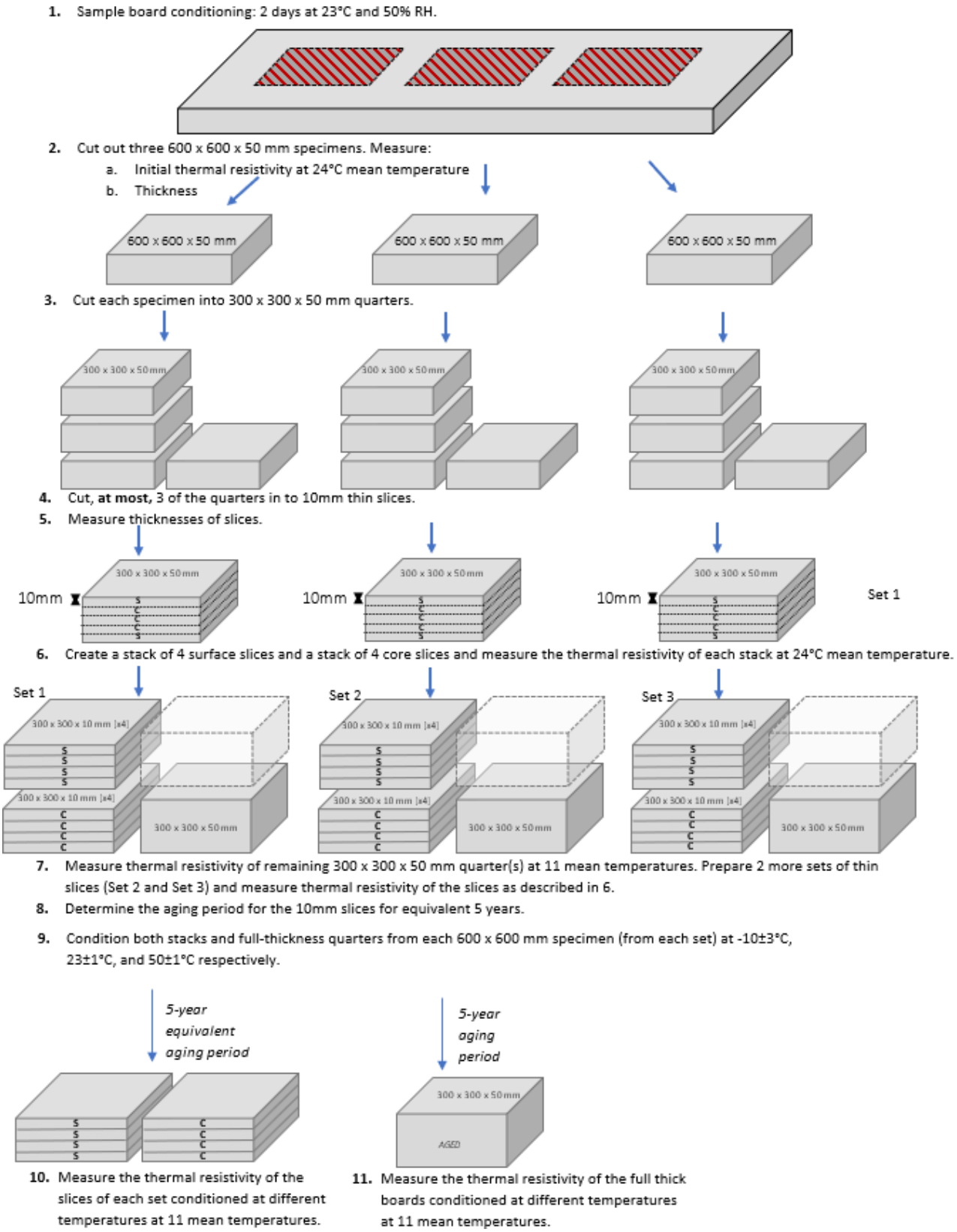

Figure 1: Testing procedure

CALCULATION METHODS

The list of all the symbols, abbreviations, and variables that are not described at the equations are listed in Table 3.

Table 3: List of abbreviations and symbols

Symbol	**Meaning**
LTTR	Long-term thermal resistivity as defined by the ULC S770 test method
$LTTR_{Acc}$	Long-term thermal resistivity as defined by the ULC S770 test method and tested by the accelerated aging (slicing and scaling method)
$LTTR_{5y}$	Long-term thermal resistivity as defined by the ULC test method and tested by 5 years of aging
$LTTR_{1303}$	Long-term thermal resistivity tested by the accelerated aging (slicing and scaling method) as per the ULC S770 test method and the LTTR is calculated as per the ASTM C1303 calculation method
$TDLTTR_{Acc}$	Temperature dependent thermal resistivities obtained by the λ_{eff} (T) function for thin slices (The ASTM C1045 integral method calculation is used)
$TDLTTR_{5y}$	Temperature dependent thermal resistivities obtained by the $\lambda_{f\text{-}5y(}T)$ function for the full thickness boards (The ASTM C1045 integral method calculation is used)
$r_{m\text{-}surface}$	Mean thermal resistivity of the surface slices at the testing point measured at its' respective mean temperature as per the ASTM C518 test method
$r_{m\text{-}core}$	Mean thermal resistivity of the core slices at the testing point measured at its' respective mean temperature as per the ASTM C518 test method
r_{5y}	Mean thermal resistivity of the full thickness products at 5 years measured at its' respective mean temperature as per the ASTM C518 test method

A_{5y}	The ratio between the thermal resistivity of 5-year aged full thickness product to its' initial thermal resistivity

The LTTR, $LTTR_{Acc}$, $LTTR_{1303}$, $LTTR_{5y}$, $LTTR_{1303}$, $TDLTTR_{Acc}$, $TDLTTR_{5y}$, A_{5y}, and effective aging factors will be calculated.

LTTR calculation methods

LTTR calculation methods

In the slicing and scaling method, the aging of the foam is assumed to be only by diffusion of BAs. So, the scaling equation (Equation 1) can be used to relate the diffusion path length and the time of aging assuming that the diffusion coefficients of the gases inside the closed-cells and the initial partial pressures are the same for full thickness boards and the sliced specimens. The testing point, t_1 is the point at which the slices achieve the same degree of aging to an equivalent time of t_2 when the thickness of the sliced specimen is L_1 and the thickness of the full thickness product is L_2.

To determine the testing point of the 10 mm thin slices, the scaling equation (Equation 1) was used.

Equation 1 $$\frac{t_1}{t_2} = \left[\frac{L_1}{L_2}\right]^2$$

In CAN/ULC S770 test method, an aging factor is determined to calculate the long-term thermal resistance. First, the aging factors (A) are determined for the core slices and the surface slices separately by taking the ratio of the thermal resistivity of the slices at the testing point (r_{tp}) to the initial thermal resistivity of the slices (r_i) (Equation 2).

Equation 2 $A = \frac{r_{tp}}{r_i}$

The effective aging factor for the full thickness product (A_{eff}) is determined by combining the aging factor for the cores (A_c) and the aging factor for the surfaces (A_s) based on their thickness contribution to the full product. Equation 3 shows the equation for the effective aging factor where L_s and L are the mean thickness of the surface slices and the mean thickness of the full thickness product respectively.

Equation 3 $A_{eff} = \left(\frac{2L_s}{L}\right)A_s + \left(\frac{L-2L_s}{L}\right)A_c$

The $LTTR_{Acc}$ is then calculated by multiplying the initial thermal resistivity of the full thickness board by the effective aging factor as given in Equation 4, where r_{i_full}.

Equation 4 $LTTR_{Acc} = A_{eff}.r_{i\_full}$

The $LTTR_{1303}$ is calculated by Equation 5, where λ_{s_tp} and λ_{c_tp} are the mean thermal conductivity of the surface slices and the mean thermal conductivity of the core slices respectively.

Equation 5

$$LTTR_{1303} = \frac{2L_s}{\lambda_{s\_tp}} + \frac{1-2L_s}{\lambda_{c\_tp}}$$

A flow chart of the calculation procedure for one material is given in Figure 2.

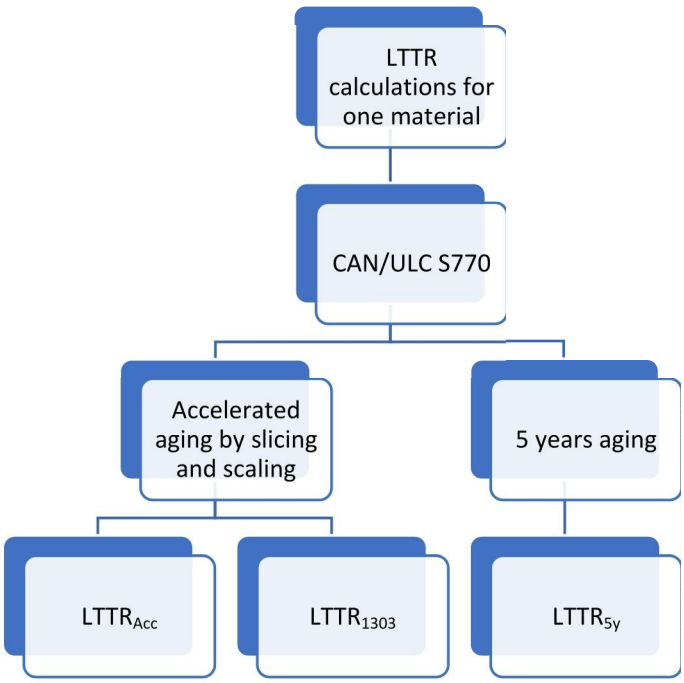

Figure 2:The flow of LTTR calculations

TDLTTR calculation methods

The thermal integration method as per ASTM C1045 was used to calculate the temperature dependent thermal conductivity. It defines the temperature dependent thermal conductivity, (T) as a third order polynomial function of temperature as shown in Equation 6.

Equation 6 $$\lambda(T) = a_0 + a_1 T + a_2 T^2 + a_3 T^3$$

When this function is integrated over the experimental temperature range (i.e., cold (T_c) and hot (T_h) plate temperature of the heat flow meter test), the thermal conductivity at the mean temperature (λ_m) can be obtained as follows Equation 7.

Equation 7 $$\lambda_m = a_0 + \frac{a_1(T_c + T_h)}{2} + \frac{a_2({T_c}^2 + T_c T_h + {T_h}^2)}{3} +$$

$$\frac{a_3(T_c{}^2 + T_h{}^2)(T_c + T_h)}{4}$$

When the thermal conductivity is measured at multiple mean temperatures, the coefficients, a_0-a_3 can be determined by least square fitting.

The steps of calculation are as follows;

- For thin slices at the testing point,

1. Determination of the temperature-dependent thermal conductivity function for surface slices, $\lambda_{sa}(T)$
2. Determination of the temperature dependent thermal conductivity function for core slices, $\lambda_{ca}(T)$
3. Determination of the effective temperature-dependent thermal conductivity for the thin slices by combining $\lambda_{sa}(T)$ and $\lambda_{ca}(T)$ by using the standard series equation (Equation 8) for the thermal resistance which is similar to Equation 5 as in ASTM C1303 calculation method.
4. At the tested mean temperatures, $\lambda_{eff}(T_x)$ is calculated (Equation 8), where T_x is the temperature value used for the calculation. The mean temperatures of the test were used as T_x.

Equation 8 $$R_{total} = \frac{L_{product}}{\lambda_{eff}(T_x)} = \frac{2L_{surface}}{\lambda_{sa}(T_x)} + \frac{1-2L_{surface}}{\lambda_{ca}(T_x)}$$

5. The temperature dependent effective thermal conductivity function, was then determined, $\lambda_{eff}(T)$.

- For the full thickness specimens initially and at 5 years,

1. Determination of the temperature dependent thermal conductivity for full thickness specimens initially, $\lambda_{\text{f-i}}(T)$
2. Determination of the temperature dependent thermal conductivity for the full thickness 5-year aged specimens, $\lambda_{\text{f-5y}}(T)$

Error/Bias calculation – Equations for bias calculations

The error/bias of the calculations were determined by calculating the difference between the estimated thermal resistivity value by the accelerated aging and the actual measured thermal resistivity at 5 years of aging as given in the Equation 9. A positive value in the bias means that the accelerated test overpredicts the actual value, and a negative value in the bias means that it underpredicts the actual value.

Equation 9

$$Bias = \frac{Thermal\ resistivity\ obtained\ by\ the\ accelerated\ testing - Thermal\ resistivity\ obtained\ by\ 5-years\ of\ aging}{Thermal\ resistivity\ obtained\ by\ 5-years\ of\ aging} \times 100\%$$

Or $Bias = \frac{LTTR_{acc} - LTTR_{5y}}{LTTR_{5y}}$ or $Bias = \frac{r_{acc} - r_{5y}}{r_{5y}}$

The flow of TDLTTR calculations is shown in Figure 3.

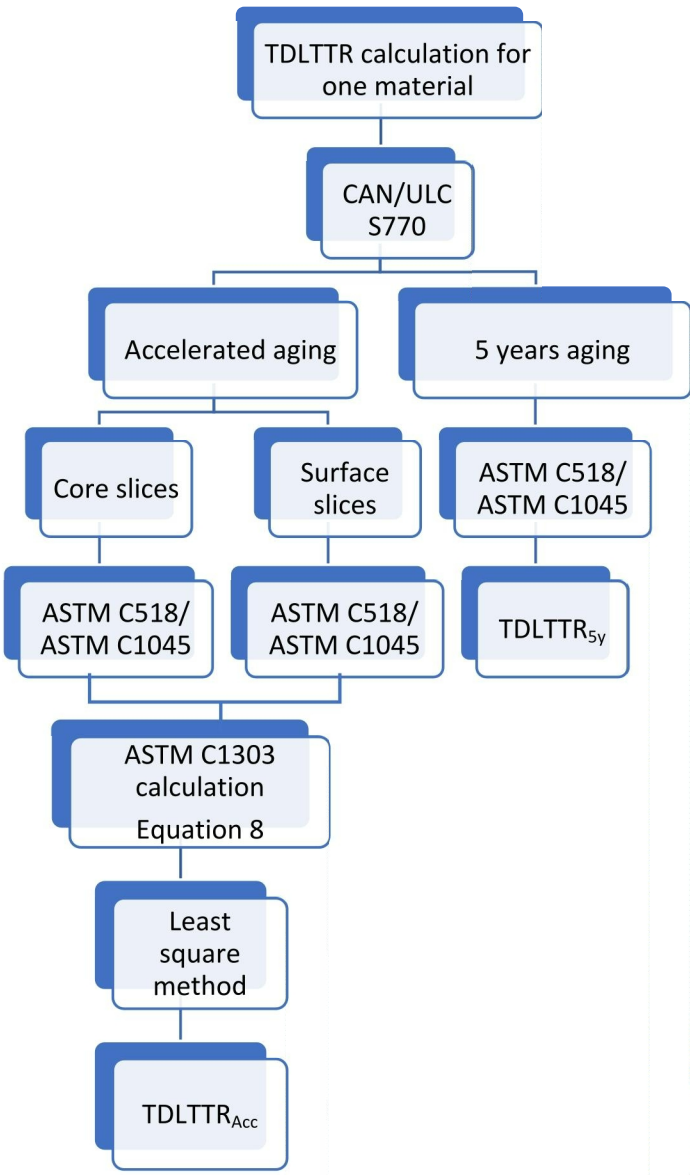

Figure 3:The flow of TDLTTR calculations

Results and Discussion

THE EFFECT OF CONDITIONING TEMPERATURES ON LTTR OF INSULATIONS AS DEFINED BY ULC S770 (SLICING AND SCALING METHOD)

Figure 4 shows the LTTR results obtained from the ULC/S770 method in comparison with the initial thermal resistivity and the thermal resistivity of the 5 years aged boards for PIR I, PIR

II, PIR III, XPS, and MDSPF. The results of PIR I, PIR II, PIR III, XPS were presented at IBPC 2024 conference and published in its proceedings[17]. It is expected that the diffusion process of the blowing agents to be slowed at the temperature below the ambient conditions and to be accelerated at the temperature above the ambient conditions. As expected, for the most of the materials tested, the thermal resistivity of the 5 years aged boards decreases with increasing conditioning temperature. This indicates that the diffusion process of the BAs is affected by the conditioning temperature.

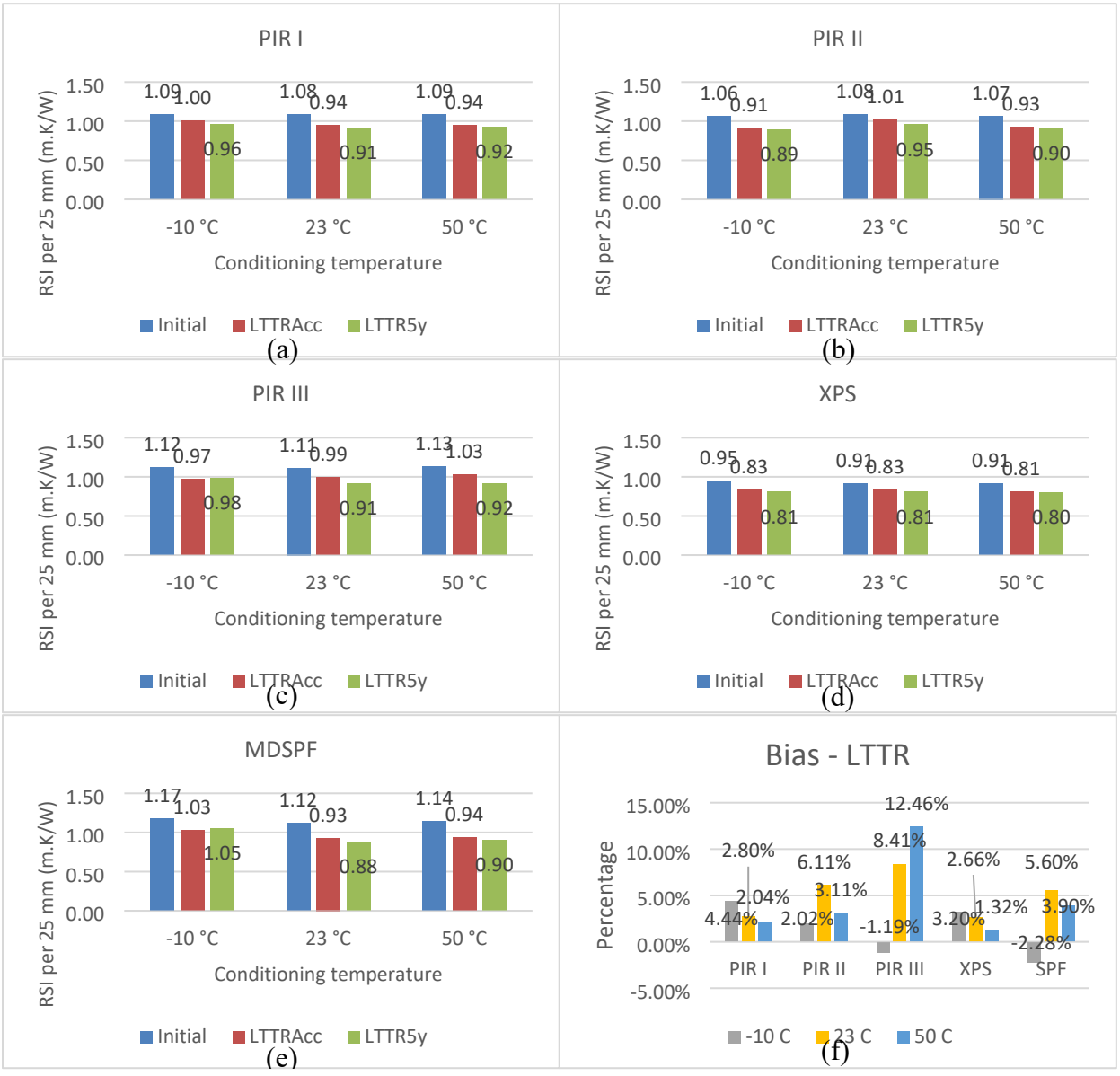

Figure 4: Effect of the conditioning temperature on the LTTR

However, the conditioning at 23 °C and 50 °C showed similar results for 5-year aged full boards for all materials except PIR II. For PIR II, the difference in the thermal resistivity of the 5-year aged full boards conditioned at 23 °C and those of conditioned at 50 °C is 5.7%, while the other materials have a difference of less than 2.2%. The $LTTR_{Acc}$ of the samples conditioned at 23 °C and 50 °C also showed a similar behaviour for materials except PIR II. For PIR II, the difference in $LTTR_{Acc}$ for conditioning at 23 °C and 50 °C is 8.5% while the other materials show a difference of less than 3.8%.

Having similar results for either $LTTR_{Acc}$ (when conditioned at 23 °C and 50 °C) or for $LTTR_{5y}$ (when conditioned at 23 °C and 50 °C) indicates that the BAs have diffused out from the foam and the BAs have been replaced by the air or they have very similar gas compositions in the cells when they are conditioned above 23 °C for 5 years or for 5-year equivalent in the accelerated testing. The results agree with research findings from Zarr and Nguyen[18] in which they observed aging at 60 °C and 10% RH and aging at 22 °C and 40 % RH resulted in a similar thermal conductivity increase for 26. 9 mm thickness PIR specimens after 372 days.

When the samples were conditioned at -10 °C, the decrease in $LTTR_{5y}$ (results of 5 years aged full thickness boards) compared to those conditioned at 23 °C is less for PIR I, PIR III, and MDSPF as expected. This validates the expectation that the conditioning in the colder temperature slows down the diffusion process for these three materials. However, the diffusion of the cell gases in XPS, does not appear to be affected by the conditioning temperature. It could be that all the BAs have diffused out and the air have diffused in to an equilibrium by the 5 years and equivalent 5-years, or the rates of the diffusion processes are not significantly affected by the conditioning temperature. The slowing down of the diffusion process at -10 °C also be observed for the

accelerated testing for PIR I and MDSPF. The results on the effect of the conditioning temperature on the aging for the XPS materials align with the research outcomes of Alvey et al.[19]. Their study of aging 50. 8 mm and 54.0 mm XPS at 90% RH and 65.6 °C, and 90% RH and 32.2 °C for 5 weeks did not show a significant difference in the aged thermal conductivity of the materials.

The $LTTR_{5y}$ for PIR II deviates from this behaviour. A trend for the effect of the conditioning temperature on the $LTTR_{5y}$ is not visible, and the effect may not be significant enough to be observed. The results suggest that the differences could be due to variations in the initial thermal resistivity of the specimens, which can be observed in both accelerated testing and 5-years aging test. (See section – **COMPARISON OF LTTRACC, LTTR1303, AND LTTR5Y**).

The graph (f) of Figure 4 shows the bias of the $LTTR_{Acc}$ towards the $LTTR_{5y}$ at each conditioning temperature. Except two incidences out of 15, the $LTTR_{Acc}$ results in an overestimation of the $LTTR_{5y}$. As discussed before the accelerated testing of PIR II and PIR III shows higher biases towards the 5 years aged values, deviating from the anticipated behavior due to the impact of the conditioning temperature. This could be related to the solubility of the BAs which may occur during the first ~70 days and might not be accounted for in accelerated testing, while the results of the full thickness boards are attributed to the remainder of the BAs that have completed dissolving. Conditioning at -10 °C shows the lowest bias, and conditioning at 50 °C for PIR III shows the highest bias for the LTTR at a 24 °C mean temperature. However, the trends in bias are different for each material.

TEMPERATURE DEPENDENT THERMAL RESISTIVITY

The polynomial coefficients of the thermal conductivity functions for $\lambda_{f\text{-}i}(T)$, $\lambda_{sa}(T)$, $\lambda_{ca}(T)$, $\lambda\_eff\ (T)$, and $\lambda f\text{-}5y(T)$ are given in Table 4.

Table 4:Polynomials of thermal conductivity functions

Material	Conditioning temperature	Temperature dependent thermal conductivity function	a_3	a_2	a_1	a_0
PIR I	-10 °C	$\lambda_{f\text{-}i}(T)$	-5.000E-08	9.554E-06	-3.001E-04	2.475E-02
		$\lambda_{ca}(T)$	-1.037E-07	1.187E-05	-2.790E-04	2.540E-02
		$\lambda_{sa}(T)$	-8.753E-08	1.050E-05	-2.477E-04	2.543E-02
		$\lambda_{eff}(T)$/ $TDLLTR_{Acc}$	-9.719E-08	1.132E-05	-2.664E-04	2.541E-02
		$\lambda_{f\text{-}5y}(T)$/ $TDLLTR_{5y}$	-1.483E-07	1.543E-05	-2.991E-04	2.602E-02
	23 °C	$\lambda_{f\text{-}i}(T)$	-3.464E-08	9.550E-06	-3.446E-04	2.558E-02
		$\lambda_{ca}(T)$	-9.946E-08	1.034E-05	-2.080E-04	2.577E-02
		$\lambda_{sa}(T)$	-8.876E-08	9.789E-06	-2.048E-04	2.640E-02
		$\lambda_{eff}(T)$/ $TDLLTR_{Acc}$	-9.539E-08	1.013E-05	-2.068E-04	2.601E-02
		$\lambda_{f\text{-}5y}(T)$/ $TDLLTR_{5y}$	-1.152E-07	1.334E-05	-3.095E-04	2.814E-02
	50 °C	$\lambda_{f\text{-}i}(T)$	-2.818E-08	8.874E-06	-3.143E-04	2.519E-02
		$\lambda_{ca}(T)$	-7.226E-08	7.984E-06	-1.534E-04	2.582E-02
		$\lambda_{sa}(T)$	-5.046E-08	6.975E-06	-1.678E-04	2.641E-02
		$\lambda_{eff}(T)$/ $TDLLTR_{Acc}$	-6.367E-08	7.585E-06	-1.590E-04	2.605E-02
		$\lambda_{f\text{-}5y}(T)$/ $TDLLTR_{5y}$	-1.200E-07	1.354E-05	-3.382E-04	2.874E-02
PIR II	-10 °C	$\lambda_{f\text{-}i}(T)$	-2.219E-08	4.659E-06	-8.046E-05	2.359E-02
		$\lambda_{ca}(T)$	-5.715E-08	7.216E-06	-1.465E-04	2.611E-02
		$\lambda_{sa}(T)$	-4.097E-08	6.671E-06	-1.500E-04	2.694E-02
		$\lambda_{eff}(T)$/ $TDLLTR_{Acc}$	-5.131E-08	7.020E-06	-1.478E-04	2.642E-02
		$\lambda_{f\text{-}5y}(T)$/ $TDLLTR_{5y}$	-9.472E-08	1.107E-05	-2.261E-04	2.804E-02
	23 °C	$\lambda_{f\text{-}i}(T)$	2.060E-08	2.759E-06	-1.061E-04	2.314E-02
		$\lambda_{ca}(T)$	-3.596E-08	5.615E-06	-1.093E-04	2.402E-02
		$\lambda_{sa}(T)$	-2.841E-08	5.803E-06	-1.211E-04	2.596E-02
		$\lambda_{eff}(T)$/ $TDLLTR_{Acc}$	-3.335E-08	5.690E-06	-1.136E-04	2.475E-02
		$\lambda_{f\text{-}5y}(T)$/ $TDLLTR_{5y}$	-5.380E-08	8.946E-06	-1.806E-04	2.585E-02
	50 °C	$\lambda_{f\text{-}i}(T)$	-3.598E-08	5.493E-06	-9.239E-05	2.277E-02
		$\lambda_{ca}(T)$	-6.342E-08	7.515E-06	-1.304E-04	2.639E-02
		$\lambda_{sa}(T)$	-5.071E-08	6.558E-06	-1.162E-04	2.719E-02

		$\lambda_{eff}(T)$/ $TDLLTR_{Acc}$	-5.849E-08	7.144E-06	-1.249E-04	2.671E-02
		$\lambda_{f\text{-}5y}(T)$/ $TDLLTR_{5y}$	-1.876E-07	2.011E-05	-5.130E-04	3.065E-02
PIR III	-10 °C	$\lambda_{f\text{-}i}(T)$	-8.337E-08	9.476E-06	-1.795E-04	2.218E-02
		$\lambda_{ca}(T)$	-6.517E-08	8.367E-06	-1.694E-04	2.559E-02
		$\lambda_{sa}(T)$	-8.018E-08	9.000E-06	-1.748E-04	2.580E-02
		$\lambda_{eff}(T)$/ $TDLLTR_{Acc}$	-7.084E-08	8.605E-06	-1.715E-04	2.567E-02
		$\lambda_{f\text{-}5y}(T)$/ $TDLLTR_{5y}$	-1.489E-07	1.576E-05	-3.176E-04	2.527E-02
	23 °C	$\lambda_{f\text{-}i}(T)$	-8.774E-08	9.981E-06	-2.048E-04	2.270E-02
		$\lambda_{ca}(T)$	-7.734E-08	8.612E-06	-1.570E-04	2.473E-02
		$\lambda_{sa}(T)$	-9.966E-08	1.102E-05	-2.194E-04	2.536E-02
		$\lambda_{eff}(T)$/ $TDLLTR_{Acc}$	-8.604E-08	9.568E-06	-1.820E-04	2.499E-02
		$\lambda_{f\text{-}5y}(T)$/ $TDLLTR_{5y}$	-1.523E-07	1.511E-05	-2.797E-04	2.694E-02
	50 °C	$\lambda_{f\text{-}i}(T)$	-8.659E-08	9.591E-06	-1.856E-04	2.211E-02
		$\lambda_{ca}(T)$	-1.099E-08	5.644E-06	-2.226E-04	2.675E-02
		$\lambda_{sa}(T)$	-8.561E-08	1.063E-05	-2.607E-04	2.635E-02
		$\lambda_{eff}(T)$/ $TDLLTR_{Acc}$	-3.941E-08	7.532E-06	-2.370E-04	2.660E-02
		$\lambda_{f\text{-}5y}(T)$/ $TDLLTR_{5y}$	-1.817E-07	1.867E-05	-4.392E-04	2.924E-02
XPS	-10 °C	$\lambda_{f\text{-}i}(T)$	2.588E-08	-1.262E-06	1.236E-04	2.558E-02
		$\lambda_{ca}(T)$	-1.536E-09	3.082E-07	1.006E-04	2.762E-02
		$\lambda_{sa}(T)$	2.127E-09	1.506E-07	1.048E-04	2.795E-02
		$\lambda_{eff}(T)$/ $TDLLTR_{Acc}$	-1.332E-10	2.478E-07	1.022E-04	2.775E-02
		$\lambda_{f\text{-}5y}(T)$/ $TDLLTR_{5y}$	-2.391E-08	1.714E-06	1.010E-04	2.774E-02
	23 °C	$\lambda_{f\text{-}i}(T)$	2.693E-08	-1.530E-06	1.279E-04	2.580E-02
		$\lambda_{ca}(T)$	3.568E-09	1.115E-07	1.118E-04	2.779E-02
		$\lambda_{sa}(T)$	6.465E-09	-9.192E-08	1.234E-04	2.821E-02
		$\lambda_{eff}(T)$/ $TDLLTR_{Acc}$	4.713E-09	3.087E-08	1.163E-04	2.796E-02
		$\lambda_{f\text{-}5y}(T)$/ $TDLLTR_{5y}$	-1.564E-09	2.361E-07	1.169E-04	2.805E-02
	50 °C	$\lambda_{f\text{-}i}(T)$	2.467E-08	-1.286E-06	1.336E-04	2.572E-02
		$\lambda_{ca}(T)$	1.460E-09	5.665E-08	1.102E-04	2.826E-02
		$\lambda_{sa}(T)$	4.223E-09	-2.534E-08	1.174E-04	2.835E-02
		$\lambda_{eff}(T)$/ $TDLLTR_{Acc}$	2.551E-09	2.387E-08	1.131E-04	2.829E-02

		$\lambda_{f\text{-}5y}(T)$/ $TDLLTR_{5y}$	-2.676E-08	1.886E-06	1.022E-04	2.818E-02
SPUF	-10 °C	$\lambda_{f\text{-}i}(T)$	-2.250E-08	2.486E-06	2.312E-05	1.957E-02
		$\lambda_{ca}(T)$	-3.970E-08	3.988E-06	-6.832E-06	2.380E-02
		$\lambda_{sa}(T)$	-3.473E-08	3.915E-06	-1.964E-05	2.289E-02
		$\lambda_{eff}(T)$/ $TDLLTR_{Acc}$	-3.736E-08	3.954E-06	-1.282E-05	2.339E-02
		$\lambda_{f\text{-}5y}(T)$/ $TDLLTR_{5y}$	-4.850E-08	5.073E-06	-2.711E-05	2.172E-02
	23 °C	$\lambda_{f\text{-}i}(T)$	-1.818E-08	2.224E-06	2.812E-05	2.050E-02
		$\lambda_{ca}(T)$	-4.200E-08	4.125E-06	-6.547E-06	2.517E-02
		$\lambda_{sa}(T)$	-3.444E-08	3.399E-06	1.669E-05	2.594E-02
		$\lambda_{eff}(T)$/ $TDLLTR_{Acc}$	-3.881E-08	3.821E-06	3.160E-06	2.550E-02
		$\lambda_{f\text{-}5y}(T)$/ $TDLLTR_{5y}$	-4.514E-08	4.004E-06	2.362E-05	2.583E-02
	50 °C	$\lambda_{f\text{-}i}(T)$	-2.338E-08	2.568E-06	2.528E-05	2.005E-02
		$\lambda_{ca}(T)$	-2.327E-08	2.598E-06	2.196E-05	2.678E-02
		$\lambda_{sa}(T)$	-3.195E-08	3.271E-06	1.072E-05	2.565E-02
		$\lambda_{eff}(T)$/ $TDLLTR_{Acc}$	-2.731E-08	2.911E-06	1.677E-05	2.627E-02
		$\lambda_{f\text{-}5y}(T)$/ $TDLLTR_{5y}$	-6.054E-08	5.147E-06	-3.460E-06	2.558E-02

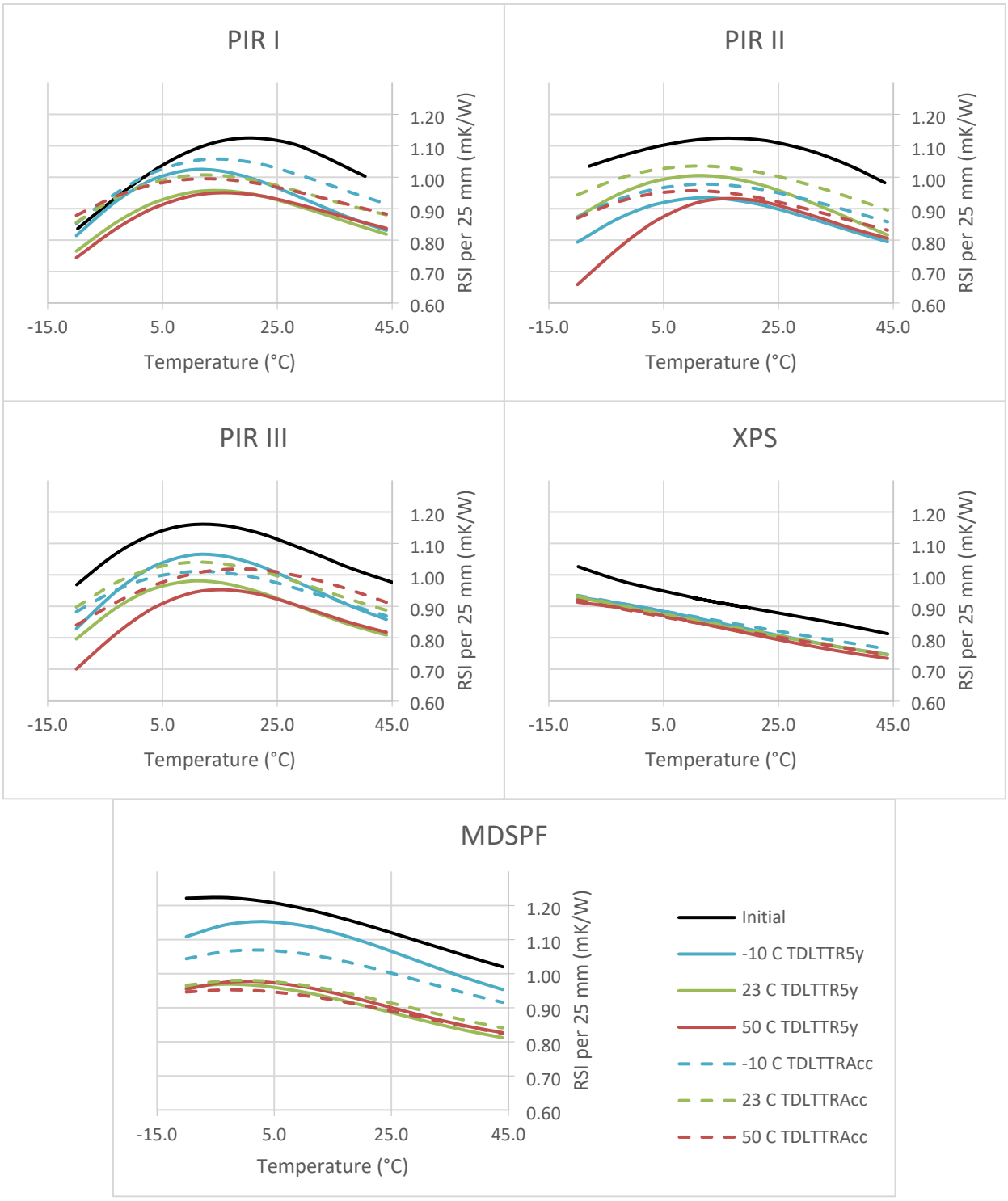

Figure 5:Temperature dependent thermal resistivity

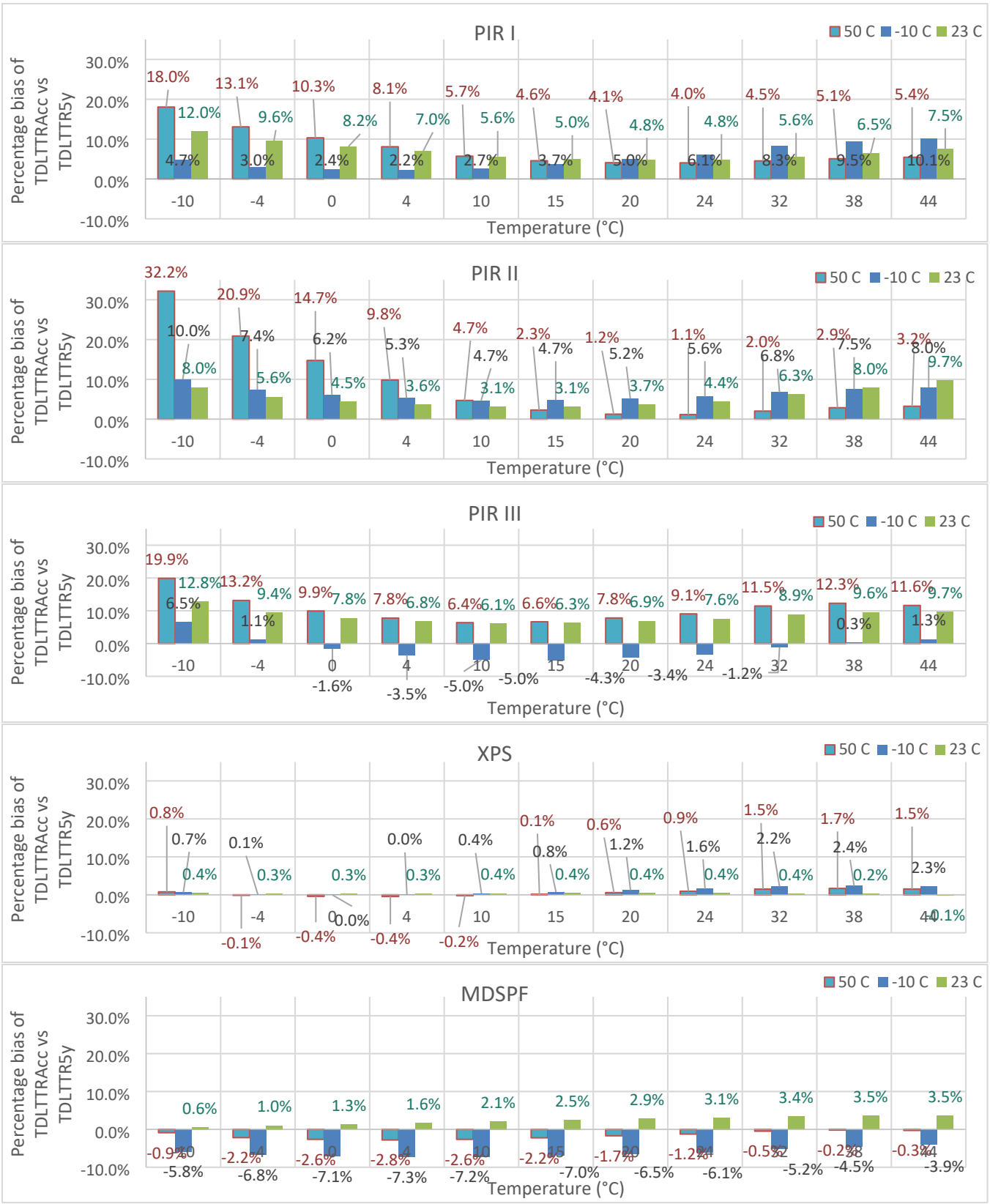

Figure 6: The bias of TDLTTR

Figure 5 shows the temperature dependent thermal resistivity per 25 mm of PIR I, PIR II, PIR III, XPS, and MDSPF conditioned at -10 °C, 23 °C, and 50 °C in comparison to the temperature dependent initial thermal resistivity per 25 mm. The results of PIR I, PIR II, PIR III, and XPS were presented at IBPC 2024 conference and published in its proceedings [17]. Each graph includes the thermal resistivities of the 5 years aged full thickness boards (solid line: $TDLTTR_{5y}$) and their thermal resistivities obtained by the accelerated testing (dashed line: $TDLTTR_{Acc}$). The curve representing the initial thermal resistivity for each material is the initial temperature-dependent thermal resistivity of the specimen that was conditioned at 23 °C.

All the materials except XPS show a non-linear behaviour for the thermal resistivity vs temperature. As the specimen mean temperature decreases, the thermal resistivity of the materials increases linearly, then starts a non-linear increase up to a maximum, and then starts decreasing. The point where the thermal resistivity starts the non-linear behaviour indicates the condensation starting point for the foam's BA. However, for XPS, the thermal resistivity kept increasing linearly as the specimen mean temperature of the test decreases. Also, this is evident in the curve for the initial TDLTTR of XPS. This indicates that the condensation of the BAs in the XPS did not occur at the tested temperature range.

It is observed that for PIR I and PIR II, the point where condensation begins shifts towards a colder temperature for the accelerated testing and the 5-year aged testing compared to that of the initial thermal resistivity curve. This indicates that the composition of gas inside the closed cells/BAs have changed due to the diffusion process and gas solubility. This could be attributed the initial solubility of BAs inside the closed cells.

Similar to the effect of conditioning temperature on the LTTR results, the conditioning temperatures affected the TDLTTR in accelerated testing and the 5-year aged testing. Except for

PIR II, conditioning at -10°C appears to have slowed down the thermal aging process, and conditioning at 50 °C appears to have accelerated the thermal aging process compared to conditioning at 23 °C. All the $TDLTTR_{Acc}$ tests showed overpredictions of the $TDLTTR_{5y}$ except for PIR III and MDSPF conditioned at -10 °C. The overprediction could be due to the solubility of BAs in the polymer matrix, which was not taken into account in the slicing and scaling method, and due to the dimensional changes in the foam observed in 5-year aged specimens. An expansion of the thickness of the specimens was observed, and due to the expansion, crease lines were present near the knit lines of the specimen for the paper-faced PIR materials. This may have a slight impact on the 5-year thermal resistivity of the full thickness PIR specimens. Additionally, MDSPF showed expansions in thickness and warpage in full thickness specimens conditioned at 23 °C and 50 °C, while the specimen conditioned at -10 °C did not show thickness changes or warpage; Regardless of that, the highest bias in the accelerated testing is from the specimens conditioned at -10 °C. So, the effect of the dimensional changes on the bias of the accelerated testing can be considered minimal.

The $TDLTTR_{5y}$ of all the materials conditioned at 50 °C appears to have the lowest thermal resistance or very close to the lowest thermal resistance out of the temperature-dependent thermal resistance curves of the materials. For PIR II and PIR III, the $TDLTTR_{5y}$ curves show a sharper decline than the others at mean temperatures below the curves' turning points. This suggests that the specimens attributed to these curves have more condensation in the cells, which seems to contradict the hypothesis that BAs have diffused completely out of the cells. So, it is possible that moisture could have diffused into the cells, causing more condensation. Additionally, at 50 °C, the air can hold more moisture than at 23 °C. Therefore, the air that diffused into the foam conditioned at 50 °C may contain more moisture than the air that was conditioned at 23°C. This can explain

the TDLTTR5y of PIR II and PIR III. This aligns with Murphy's statement that the aging of foam greatly depends on its immediate environment, including the equilibrium moisture content of the facers[2]. Materials with facers show a relatively higher bias than XPS and MDSPF in the temperature-dependent thermal resistance of the specimens conditioned at 23 °C and 50 °C. Conditioning at -10 °C affected the accelerated testing and 5-year aging tests in different ways, including shifts in the points related to the beginning of the condensation.

Figure 6 presents the bias of the $TDLTTR_{Acc}$ compared to the $TDLTTR_{5y}$. Overall, the bias in the accelerated testing increased at the extreme ends of the tested temperature ranges. For PIR, the bias trends appear similar and more significant at the mean temperatures of the experiments compared to the other materials. The bias percentages at colder mean temperatures are greater for the materials (PIR I and II) conditioned at 50 °C. However, for materials conditioned at -10 °C, the increase in bias at colder temperatures is less pronounced. This may be due to enhanced solubilization of the BAs at higher temperatures. The thin slices may not exhibit the same level of solubilization because the solubilization period is shorter in them compared to the materials conditioned for 5 years. Previous research on the thermal aging of polyurethane [20, 21, 22] has shown impact of BA solubility and the adsorption and desorption of BAs into the polymer matrix on thermal aging. Therefore, this should be considered, even though the LTTR test methods used in this study do not account for it. It is recommended to analyze the cell gases to better understand what occurs during temperature changes. The bias of these curves is approximately 10% or below for mean temperatures around 0 °C or above. However, the bias increases significantly when the mean temperature of the tests is below that point. This substantial decrease in the thermal resistivity of the 5-year aged samples ($TDLTTR_{5y}$) suggests that moisture may be present inside these materials, and condensation of moisture could be causing this effect. The

reason it is not visible in the accelerated testing may be that the samples in the accelerated tests did not reach equilibrium adsorption, while the 5-year aged samples had sufficient time to do so. As previously noted, the bias is greater in materials with facers than in those without.

Materials conditioned at 23 °C or 50 °C show positive biases, while negative biases result only from materials conditioned at -10 °C. It is possible that all the BAs condensed in the cells initially, while diffusion processes affected other gases. Therefore, outward diffusion of BAs should be less pronounced in materials conditioned at -10°C. However, in materials conditioned at 23 °C or 50 °C, both inward and outward diffusion could occur.

Furthermore, XPS, which did not show nonlinear temperature dependency in thermal resistivity, exhibited the lowest bias. Condensation of BAs is not visible in this material, suggesting that the boiling point of the BAs is lower.

AGING FACTORS

Table 5: Aging factors and Bias at 24C Mean Temperature

	-10 °C			23 °C			50 °C		
	A_{acc}	A_{5y}	Bias	A_{acc}	A_{5y}	Bias	A_{acc}	A_{5y}	Bias
PIR I	0.920	0.865	6.43%	0.872	0.826	5.63%	0.869	0.835	4.07%
PIR II	0.861	0.859	0.20%	0.937	0.861	8.79%	0.870	0.839	3.74%
PIR III	0.857	0.877	-2.33%	0.884	0.821	7.64%	0.908	0.810	12.09%
XPS	0.944	0.910	3.78%	0.928	0.915	1.40%	0.918	0.910	0.92%
MDSPF	0.845	0.897	-5.75%	0.780	0.784	-0.41%	0.789	0.787	0.22%

Table 5 shows the aging factors for the mean temperature of 24°C of the tested materials. The aging factor calculated by the ULC S770 testing method is used for the aging factor of the accelerated testing (A_{Acc}). The aging factors for the 5 years aging was calculated by the ratio of

the thermal resistivity of the specimen at 5 years aging to the its' initial thermal resistivity. There were instances where the initial thermal resistivity was not recorded exactly at 24 °C mean temperature (For example, it was recorded at 24.1 °C; at a value close to 24 °C). For those specimens the initial mean thermal resistivity was calculated using Equation 7. The coefficients were used from its relevant calculated function for initial thermal conductivity ($\lambda_{f\text{-}i}(T)$). When comparing the aging factors of the 5 years aged specimens conditioned at 23 °C and 50 °C, the results show that thermal aging at both 23 °C and 50 °C ends up in similar results. The maximum difference is 2.6% which is from PIR II. This indicates that either the BAs have diffused out of the foam to the same level in both cases or all the BAs have diffused out of the foam. When the aging factors are calculated by the accelerated testing, the difference between the aging factors (A_{Acc}) of the materials conditioned at 23 °C and 50 °C, is less than 2.7% for four materials, PIR I, PIR III, XPS, and MDSPF. PIR II has a difference of 7.1% for the aging factors (A_{Acc}) of materials conditioned at 23 °C and 50 °C. Overall, it could be inferred that for these four materials, conditioning at 23 °C and 50 °C affect the material same way in both accelerated and 5 years aging test.

When comparing the aging factors of the full thickness boards conditioned at -10 °C from the 5 years aging tests, it shows that three materials (The difference between the aging factors of full thickness boards conditioned at -10°C and 23°C is 5% for PIR I, 0% for PIR II, and -1% for XPS.) thermally aged to a similar extent when conditioned at -10 °C and 23 °C. However, only XPS out of them, showed similar thermal aging in accelerated testing. When the material is being conditioned at -10 °C, at least a part of BAs should be in the liquid state for the materials that show a non-linear temperature dependent thermal conductivity. So, the solubilization of the BAs also affects the thermal aging of the material which makes the predicting the LTTR difficult when they

are conditioned at -10 °C.

However, the accelerated testing show biases towards the 5 years aging test. Most of the time, the aging factor is overpredicted by the accelerated testing indicating that diffusion alone cannot predict the thermal aging of the closed-cell polymers.

COMPARISON OF $LTTR_{ACC}$, $LTTR_{1303}$, AND $LTTR_{5Y}$

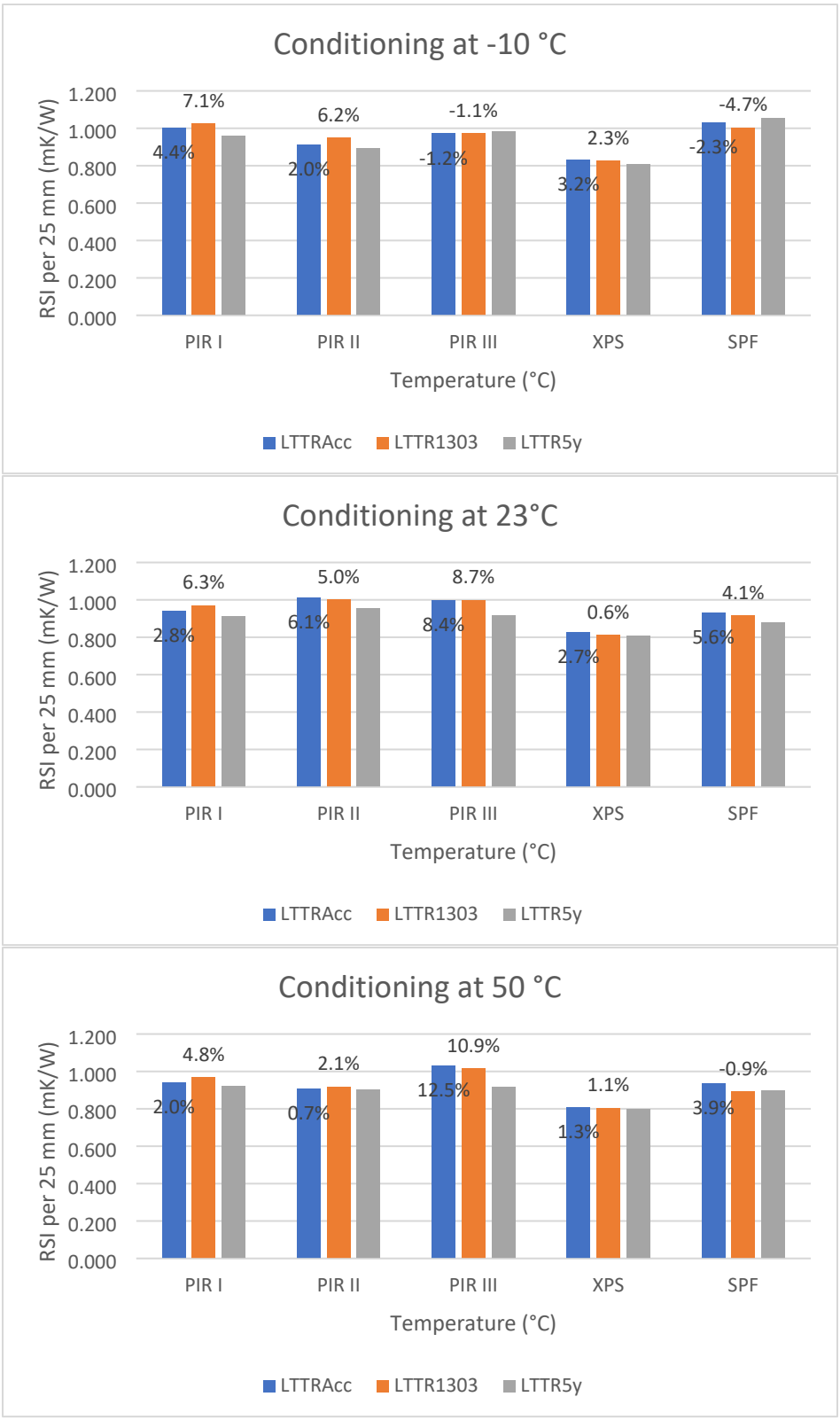

Figure 7: Comparison of LTTR1303, LTTRAcc, LTTR5y

Figure 7 shows LTTR results of the materials calculated by the ULC S770 method and the ASTM C1303 method compared with the LTTR of the 5-year aged materials. The bias of the results is calculated with reference to the 5-year aged full thickness boards and for conditioning at -10 °C, 23 °C, and 50 °C. The numbers in the respective bar relate to their bias towards the LTTR results obtained after 5 years of aging. When samples are conditioned at 23°C, the LTTR results calculated according to the ULC S770 method and the ASTM C1303 method are comparable. Regardless of the calculation method, PIR III shows the highest bias in the LTTR results when the specimens are conditioned at 23°C. The maximum difference between the biases of the two methods is 3.4% for PIR I, and for the remaining materials, the difference between the biases is less than 2.0% (when conditioned at 23°C).

The difference between the two calculation methods is that the ULC method takes the initial thermal resistance into consideration while the ASTM method does not. The ULC method considers the initial thermal resistivity of the full panel (600 mm x 600 mm) while aging is calculated only for 300 mm x 300 mm slices of the panel. The ASTM method considers only the thermal resistance of the aged slices. In the ULC test method, the initial thermal resistivity of the slices is measured within 2 hours of cutting. Therefore, the initial thermal resistivity of the slices may be slightly less than the initial thermal resistivity of the full thickness products. This should result in a slightly higher value for $LTTR_{Acc}$ than for $LTTR_{1303}$ if the initial thermal resistivities of slices and the full thickness boards are different. This can be observed for PIR II, XPS, and MDSPF. However, considering the LTTR values for the other materials, it is difficult to conclude that the difference is solely due to the difference in initial thermal resistivity. It could also be due to variations in thermal resistivity throughout the panel for a material.

When conditioning at 50 °C, which is associated with the accelerated testing, the maximum

difference between $LTTR_{Acc}$ and LTTR1303 is 4.7% for MDSPF. The other materials show differences below 2.8%. The maximum difference in biases for $LTTR_{Acc}$ and $LTTR_{1303}$ is 4.0% when the samples were conditioned at -10°C for PIR II. The only factor that affects the difference in $LTTR_{Acc}$ and $LTTR_{1303}$ is the initial thermal resistivity of the slices and the full thickness products, even when the specimens are conditioned at different temperatures. In all cases, the maximum difference between $LTTR_{Acc}$ and $LTTR_{1303}$ is 4.7% (MDSPF), and $LTTR_{Acc}$ is not always greater than $LTTR_{1303}$. This again suggests that the difference comes from the thermal resistivity variation throughout the panel for a material; test methods CAN/ULC S770 and ASTM C1303 require a certain degree of foam homogeneity throughout material thickness, which may not be sufficient.

The ASTM C1303 test method requires “homogeneity qualifications” for a material to be tested by the prescriptive method in order to determine the applicability of the test method. Even though this study used the ASTM C1303 calculation method, it did not assess this qualification of the material. Stovall et al.[23] highlighted the need for homogeneity in foam insulations to accurately predict the LTTR values and suggested assessing the homogeneity of a new formulation using a criterion in their ruggedness tests. Bogdan et al.[24] studied the CAN/ULC S770 method and ASTM C1303 for PIR with different blowing agents. They tested PIR with 1.5”, 2.0”, and 2.7” thicknesses and found out that the difference between the test results increases as the thickness of the material increases[24]. However, their test method for the CAN/ULC S770 was an older version where the effective aging factors was selected as the higher aging factor out of the aging factors for cores and surfaces[24].

ASTM C1045 CALCULATION METHOD IN THE ACCELERATED TESTING FOR THE MATERIALS CONDITIONED AT 23 °C

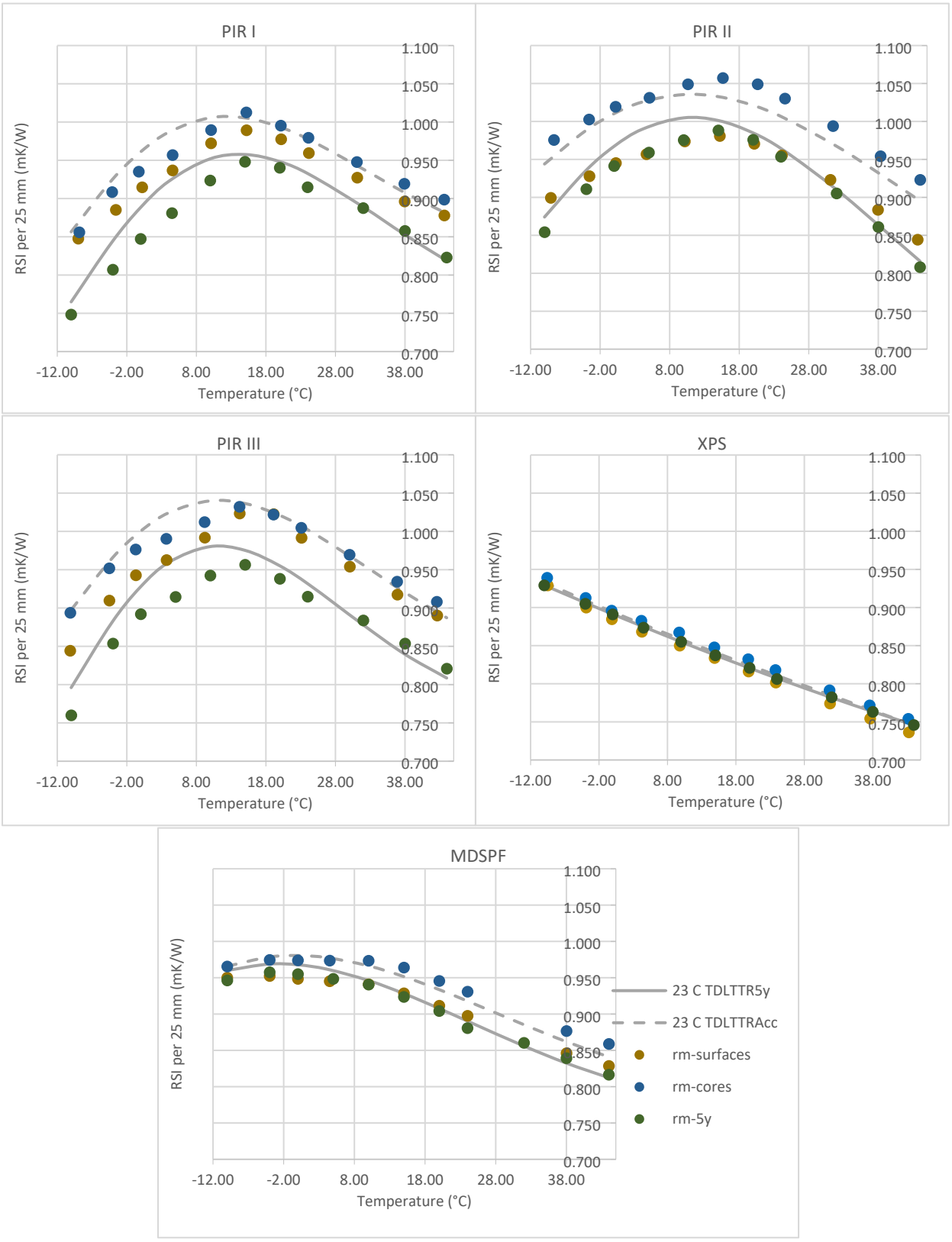
PIR I
PIR II
PIR III
XPS
MDSPF
RSI per 25 mm (mK/W)
Temperature (°C)
1.100
1.050
1.000
0.950
0.900
0.850
0.800
0.750
0.700
-12.00
-2.00
8.00
18.00
28.00
38.00
23 C TDLTTR5y
23 C TDLTTRAcc
rm-surfaces
rm-cores
rm-5y

Figure 8: Temperature dependent thermal resistivity by the ASTM C1045 calculations

Figure 8 shows the $TDLTTR_{Acc}$, $TDLTTR_{5y}$, the mean thermal resistivity of cores ($r_{m\text{-}cores}$) and surfaces ($r_{m\text{-}surfaces}$) at the testing point, and the mean thermal resistivity of 5-year aged full thickness boards ($r_{m\text{-}5y}$) for the specimens conditioned at 23 °C. The curves related to the $TDLTTR_{5y}$ and the mean thermal resistivity of the 5-year aged full boards show that the mean thermal resistivity values and the thermal resistivity at mean temperatures are different, especially in the nonlinear sections. This also shows that in the linear sections of the graphs, the mean thermal conductivity data points lie almost on the relevant curve. XPS, which shows a linear temperature dependency, has all of the mean thermal resistivity data points on its temperature-dependent thermal resistivity curve.

A closer and separate observation of the mean thermal conductivity of the cores and surfaces from these curves depicts that the mean thermal resistivities of the surfaces are lower than those of the cores at their mean thermal temperatures. This makes the bias of the thermal resistance of the cores towards that of the full-thickness specimens higher than the bias of the surfaces. In PIR II, the mean thermal resistivity of the surfaces is very close to that of the 5-year aged full thickness specimens. So, the bias should mainly come from the core specimens in PIR II. Even though the mean thermal resistivity of surfaces is not very close to that of the full thickness specimens of other materials with facers (PIR I and PIR III), as in PIR II, the thermal resistivity of core specimens adds more bias than the thermal resistivity of the surface specimens does. However, this behavior of more aging in cores than that of in surfaces agrees with what is usually expected. The previous work of Singh et al. [4] showed a similar behaviour in PIR with facers.

CONCLUSIONS

The study of long-term thermal resistance (LTTR) of five materials PIR I, PIR II, PIR III, XPS, and MDSPF produced several key conclusions:

Conditioning temperatures significantly impact the long-term thermal performance of closed-cell foam insulations as observed from both the 5-year aging and accelerated testing. LTTR results obtained using the ULC S770 test method demonstrated that conditioning samples at -10°C slowed the thermal aging process in both accelerated and 5-year aging tests, with a bias in accelerated testing towards 5-year aging being 4.4% or less when measured at a mean temperature of 24C. Conditioning at 23°C and 50°C yielded similar LTTR values for both test types. However, the bias in accelerated testing was high for two materials, reaching up to 8.4% and 12.5% for conditioning at 23°C and 50°C, respectively. This suggests that material homogeneity and the solubility of blowing agents (BAs) significantly affect test results.

The impact of conditioning was less apparent when analyzing the aging factors from the 5-year aging test and their biases, compared to the LTTR analysis. For samples conditioned at colder temperatures, tests focused solely on the diffusion process must also account for the solubility of BAs. Assessing the homogeneity of the materials is crucial to identifying sources of bias.

The comparison between $LTTR_{Acc}$ and $LTTR_{1303}$ indicated that the two test methods produce similar results, with a maximum difference of 4.7%. Contrary to expectations, $LTTR_{1303}$ did not consistently result in smaller values than $LTTR_{Acc}$, emphasizing the necessity for homogeneity verification in the tests.

The study emphasized the need for the ASTM C1045 integral method calculations and temperature-dependent thermal resistance values to avoid errors in thermal resistivity at varying mean temperatures, particularly where the thermal conductivity behavior is nonlinear. Accurately estimating thermal resistivity requires using the ASTM C1045 integral method calculations to

determine thermal resistivity at various mean temperatures. Additionally, core slices introduced more bias in accelerated testing than surface slices, especially for materials with facers. Inward moisture diffusion in the materials is another factor that must be considered to obtain accurate results from accelerated testing when materials with facers are tested.

Overall, the study highlights the complexity of thermal aging in closed-cell foam and emphasizes the importance of considering factors such as solubility, material homogeneity, and inward moisture diffusion in accelerated testing. Further research is recommended to explore the effects of these factors on both accelerated and 5-year aging tests.

ACKNOWLEDGEMENTS

This project was funded by Infrastructure Canada and expanded under the National Adaptation Strategy, builds upon the work completed under the Climate Resilient Buildings and Core Public Infrastructure Initiative (CRBCPI).

References

[1] T. Stovall, M. Vanderlen and J. Atchley, "Closed cell foam insulation: a review of long term thermal performance research," 2012.

[2] J. Murphy, "Long-term Aging of Closed-Celled Foam Insulation," *Cellular Polymers.,* vol. 29, no. 5, pp. 313-326., 2010;:.

[3] T. Makaveckas, R. Bliūdžius and A. Burlingis, "Determination of the impact of environmental temperature on the thermal conductivity of

polyisocyanurate (PIR) foam products," *Journal of Building Engineering,* vol. 41, no. 2021, p. 102447.

[4] S. N. Singh, M. Ntiru and K. Dedecker, "Long term thermal resistance of pentane blown polyisocyanurate laminate boards," *Journal of cellular plastics* , vol. 39, no. 4, pp. 265-280, 2003.

[5] ASTM C1303/C1303M-23, *Standard Test Method for Predicting Long-Term Thermal Resistance of Closed-Cell Foam Insulation,* PA: ASTM International, 2023.

[6] CAN/ULC S770-20, *Standard Test Method for Determination of Long-Term Thermal Resistance of Closed-Cell Thermal Insulating Foams,* Ottawa: Standards Council of Canada, 2020.

[7] International Organization for Standardization, *ISO 11561: Ageing of thermal insulation materials — Determination of the long-term change in thermal resistance of closed-cell plastics (accelerated laboratory test methods),* 1999.

[8] U. Berardi, "The impact of aging and environmental conditions on the effective thermal conductivity of several foam materials," *Energy,* vol. 182, pp. 777-794, 2019.

[9] H. Zhang, W. Z. Fang, Y. M. Li and W. Q. Tao, "Experimental study of

the thermal conductivity of polyurethane foams," *Applied Thermal Engineering* , vol. 115 , pp. 528-538., (2017): .

[10] K. Kontomaris, "HFO-1336mzz-Z: High temperature chemical stability and use as a working fluid in Organic Rankine Cycles.," in *INTERNATIONAL REFRIGERATION AND AIR CONDITIONING CONFERENCE*, 2014.

[11] F. Molés, J. Navarro-Esbrí, B. Peris, A. Mota-Babiloni, Á. Barragán-Cervera and K. K. Kontomaris, "Low GWP alternatives to HFC-245fa in Organic Rankine Cycles for low temperature heat recovery: HCFO-1233zd-E and HFO-1336mzz-Z," *Applied Thermal Engineering,* , vol. 71 , no. 1, pp. 204-212, 2014.

[12] J. R. Juhasz, "Novel working fluid, HFO-1336mzz (E), for use in waste heat recovery application.," in *12th IEA Heat Pump Conference*, May 2017.

[13] F. D. Rossini, "Pure Compounds from Petroleum," *Analytical Chemistry* , vol. 20, no. 2, pp. 110-121, 1948.

[14] National Center for Biotechnology Information, "PubChem Compound Summary for CID 6556, Isopentane.," [Online]. Available: https://pubchem.ncbi.nlm.nih.gov/compound/Isopentane.. [Accessed 11

September 2024].

[15] S. Molleti and D. Van Reenen, "Effect of temperature on long-term thermal conductivity of closed-cell insulation materials," *Buildings,* vol. 12, no. 4 , p. 425, 2022.

[16] N. Holcroft, "Temperature dependency of the long-term thermal conductivity of spray polyurethane foam," *Journal of Building Physics,* vol. 45, no. 5, pp. 571-603, 2022.

[17] D. P. A. Kodippili, S. Molleti and D. Van Reenen, "Temperature dependent long-term thermal resistance of closed-cell foam insulations," in *Proceedings of the 9th International Building Physics Conference (IBPC 2024) Volume 3: Building Systems and HVAC Technologies*, Toronto, 2024.

[18] R. R. Zarr and T. Nguyen, "Effects of Humidity and Elevated Temperature on the Density and Thermal Conductivity of a Rigid Polyisocyanurate Foam Co-Blown with CCl3F and CO 2," *Journal of Thermal Insulation and Building Envelopes,* vol. 17, no. 4, pp. 330-350, 1994.

[19] J. B. Alvey, J. Patel and L. D. Stephenson, "Experimental study on the effects of humidity and temperature on aerogel composite and foam

insulations," *Energy and Buildings* , no. 2017, pp. 358-371, 144 .

[20] M. T. Bomberg and M. K. Kumaran, "Use of the distributed parameter continuum (DIPAC) model for estimating the long-term thermal performance of insulating foams," *Cellular polymers,* vol. 14, no. 5, pp. 1-23, 1995.

[21] G. M. R. Du Cauze de Nazelle, "Thermal conductivity ageing of rigid closed cells polyurethane foams," 1995 .

[22] M. K. Kumaran, M. T. Bomberg, R. G. Marchand, M. R. Ascough and J. A. Creazzo, "A method for evaluating the effect of blowing agent condensation on sprayed polyurethane foams," *Journal of Thermal Insulation,* vol. 13, no. 2, pp. 123-137, 1989.

[23] T. K. Stovall, M. Vanderlan and J. A. Atchley, "Evaluation of experimental parameters in the accelerated aging of closed-cell foam insulation. No. ORNL/TM-2012/214," Oak Ridge National Lab.(ORNL), Oak Ridge, TN (United States), Building Technologies Research and Integration Center (BTRIC), 2012.

[24] M. Bogdan, J. Hoerter and F. O. Moore, "Meeting the Insulation Requirements of the Building Envelope with Polyurethane and Polyisocyanurate Foam," *Journal of Cellular Plastics,* vol. 41, no. 1, pp.

41-56, 2005.